

RESEARCH ARTICLE

# Recombinant sclerostin antagonizes effects of ex vivo mechanical loading in trabecular bone and increases osteocyte lacunar size

M. Kogawa,<sup>1</sup> K. A. Khalid,<sup>1</sup> A. R. Wijenayaka,<sup>1</sup> R. T. Ormsby,<sup>1</sup> A. Evdokiou,<sup>2</sup> P. H. Anderson,<sup>3</sup> D. M. Findlay,<sup>1\*</sup> and G. J. Atkins<sup>1\*</sup>

<sup>1</sup>Biomedical Orthopaedic Research Group, Centre for Orthopaedic and Trauma Research, University of Adelaide, Adelaide, South Australia, Australia; <sup>2</sup>Discipline of Surgery, Breast Cancer Research Unit, Basil Hetzel Institute, University of Adelaide, Woodville, South Australia, Australia; and <sup>3</sup>School of Pharmacy and Medical Sciences, University of South Australia, Adelaide, South Australia, Australia

Submitted 4 August 2017; accepted in final form 2 October 2017

**Kogawa M, Khalid KA, Wijenayaka AR, Ormsby RT, Evdokiou A, Anderson PH, Findlay DM, Atkins GJ.** Recombinant sclerostin antagonizes effects of ex vivo mechanical loading in trabecular bone and increases osteocyte lacunar size. *Am J Physiol Cell Physiol* 314: C53–C61, 2018. First published October 4, 2017; doi: 10.1152/ajpcell.00175.2017.—Sclerostin has emerged as an important regulator of bone mass. We have shown that sclerostin can act by targeting late osteoblasts/osteocytes to inhibit bone mineralization and to upregulate osteocyte expression of catabolic factors, resulting in osteocytic osteolysis. Here we sought to examine the effect of exogenous sclerostin on osteocytes in trabecular bone mechanically loaded ex vivo. Bovine trabecular bone cores, with bone marrow removed, were inserted into individual chambers and subjected to daily episodes of dynamic loading. Cores were perfused with either osteogenic media alone or media containing human recombinant sclerostin (rhSCL) (50 ng/ml). Loaded control bone increased in apparent stiffness over time compared with unloaded bone, and this was abrogated in the presence of rhSCL. Loaded bone showed an increase in calcein uptake as a surrogate of mineral accretion, compared with unloaded bone, in which this was substantially inhibited by rhSCL treatment. Sclerostin treatment induced a significant increase in the ionized calcium concentration in the perfusate and the release of  $\beta$ -CTX at several time points, an increased mean osteocyte lacunar size, indicative of osteocytic osteolysis, and the expression of catabolism-related genes. Human primary osteocyte-like cultures treated with rhSCL also released  $\beta$ -CTX from their matrix. These results suggest that osteocytes contribute directly to bone mineral accretion, and to the mechanical properties of bone. Moreover, it appears that sclerostin, acting on osteocytes, can negate this effect by modulating the dimensions of the lacunocanalicular porosity and the composition of the periosteocyte matrix.

sclerostin; mechanical loading; osteocyte; osteocytic osteolysis; bone mineralization

## INTRODUCTION

Bone is a metabolically active organ that undergoes continuous remodeling (20, 44), which is necessary to maintain the structural integrity of the skeleton (8, 50). A lack of loading

causes an imbalance of this remodeling, favoring bone resorption over bone formation. Accumulated evidence suggests that osteocytes play key roles in the regulation of bone remodeling by controlling the function of the other cell types in bone, such as activating osteoblastogenesis or osteoclastogenesis in response to increased or decreased strains, respectively, imposed by mechanical loading (1, 21, 22, 24, 33, 34, 42). In particular, osteocytes have a key role in mechanotransduction, the mechanism by which mechanical load applied to bone is converted to biological signals for maintaining appropriate strength and mechanical integrity of the bone (15, 16, 47). Although it is well established that loading has anabolic effects on bone, inducing endosteal and periosteal bone formation, the effects of loading on the bone matrix are less clear.

Mature osteocytes embedded in the mineralized bone matrix secrete sclerostin, the product of the sclerosteosis (*SOST*) gene (38), which is a potent anti-anabolic factor of bone formation (9, 25–27, 51, 55). The *SOST* gene appears to be mechanosensitive, with sclerostin production reported to be suppressed in a mouse ulnar loading model (45). Tu and coworkers (49) reported that cyclic ulnar loading-induced bone formation in mice did not occur in animals transgenic for human *SOST* expression, where effective sclerostin levels remained abnormally high after loading, indicating that the downregulation of sclerostin expression was a prerequisite for loading-induced bone growth. Consistent with this, Moustafa and colleagues (31) reported in a mouse tibial axial loading model that the suppression of *Sost* colocalized with regions of increased strain and increased bone formation. In contrast, *Sost* expression was reported to increase in response to unloading of bone (31, 45). Lin and coworkers (28) reported that unloading-induced bone loss was sclerostin-dependent, as *Sost-null* mice were resistant to this effect. A study by Macias and colleagues (30) suggested that the relationship between *Sost* expression and loading is more complex, as in a rat hindlimb unloading model, whereas *Sost* mRNA levels increased in diaphyseal cortical bone in response to unloading, they decreased in metaphyseal cortical and trabecular bone. Despite this, it appears that pharmacological inhibition of sclerostin prevents and reverses unloading-induced bone loss in both cortical and trabecular bone compartments, as shown in the mouse hindlimb tail suspension model (48).

\* D. M. Findlay and G. J. Atkins are joint senior authors.

Address for reprint requests and other correspondence: G. J. Atkins, Level 7, Adelaide Health and Medical Sciences (AHMS) Building, Univ. of Adelaide, North Terrace and George St., Adelaide, SA 5000, Australia (e-mail: gerald.atkins@adelaide.edu.au).

Recent evidence from our group suggests that, in bone formation, mature cells of the late osteoblast to osteocyte stages are key cellular targets for the action of sclerostin (2, 23, 54). We reported that sclerostin induced the expression of mineralization inhibitory peptides, termed MEPE-ASARM (acidic, serine, aspartate-rich, MEPE-associated) peptides, derived from the proteolytic processing of matrix extracellular phosphoglycoprotein (MEPE) (2). We also showed that sclerostin could act as a catabolic agent by stimulating osteocyte support of osteoclastic activity via the receptor-activated nuclear factor kappa-B ligand (RANKL) signaling pathway (54), which could explain the rapid and marked effect on bone resorption when sclerostin is inhibited clinically using a sclerostin-neutralizing antibody (36). We also demonstrated a direct catabolic action of sclerostin in promoting osteocytic osteolysis, increasing osteocyte expression of carbonic anhydrase II (CA2) (23), cathepsin K (CTSK), and matrix metalloproteinase-13 (MMP13). Treatment with exogenous sclerostin resulted in an increase in the size of osteocyte lacunae in human trabecular bone over 7 days in static, mechanically nonloaded culture *ex vivo* (23). Together, these findings provide evidence that sclerostin acts on osteocytes to control bone volume via bone formation and bone remodeling, and on bone matrix mineralization by regulating osteocytic osteolysis.

In this study, we further investigated the effects of sclerostin on osteocytes in the context of their natural conformation within bone matrix, largely free of other cell types and where the effects of bone loading were separated from the influence of the circulation and other organ systems. Isolated cores of cancellous bone were perfused with culture fluid and loaded using the Zetos culture/loading system (18). Although daily episodes of loading induced mineral accretion and increased apparent stiffness compared with unloaded bone, the addition of exogenous recombinant sclerostin inhibited these changes. Concomitantly, exogenous sclerostin increased the expression of bone resorption marker genes, such as *CA2* and *CTSK* mRNA and increased mean osteocyte lacunar size, indicative of osteocytic osteolysis. Our findings suggest that sclerostin can block response to mechanical loading in part via direct actions on osteocyte-controlled mineral accretion and the promotion of osteocytic osteolysis.

## MATERIALS AND METHODS

**Sample preparation and culture conditions.** Cancellous bovine bone was obtained fresh from the sternum of male cattle less than 2 yr of age courtesy of a local slaughterhouse. Using a specially designed diamond-coated hollow drill (Grizzly Industrial, Bellingham, WA), bone cores with a diameter of 10 mm were drilled out of the bone slices under sterile conditions. The bone cores were then machined to 5 mm thickness using a plane-parallel saw (5). During the entire procedure, the saw, drill, and bone were continuously cooled with sterile saline to prevent thermal necrosis and desiccation. The bone cores were washed with sterile saline using a dental cleaning device (Water Pik, Fort Collins, CO) to remove the bone marrow, and then placed in sterile bone chambers and connected to individual culture media reservoirs, at 37°C. They were perfused with the mineralizing cell culture media (7 ml/sample) consisting of Dulbecco's Modified Eagle Medium (DMEM) (Invitrogen, Carlsbad, CA) with 20 mM HEPES, 10% fetal calf serum, 1.8 mM KH<sub>2</sub>PO<sub>4</sub>, 100 μM L-ascorbate-2-phosphate, 2 mM L-glutamine, 1.2 mg/ml benzyl-penicillin, 1.6 mg/ml gentamicin sulfate, and 4 μg/ml amphotericin B, at a rate of 7 ml/h using a 24-channel planetary drive peristaltic pump (Ismatec IP

24, Ismatec SA, Switzerland). After equilibration for 24 h, bone cores were perfused in the absence or additional presence of 50 ng/ml human recombinant sclerostin (rhSCL; R&D Systems, Minneapolis, MN). The dose of 50 ng/ml rhSCL was chosen based on that we had already demonstrated to have near-maximal effects on osteoblast/osteocyte lineage cells *in vitro* (2, 54). Media with all supplements, including rhSCL where used, were changed daily throughout the experimental period and eluates stored at 4°C for analysis.

**Mechanical stimulation and measurement of stiffness.** Bone cores were loaded using a second-generation Zetos device, running proprietary software (Zetos version 2.0.0.1, Simplex Scientific). Loaded bone cores received a single episode of 300 cycles of loading per day at 2,000 microstrain at 1 Hz. The apparent stiffness measured in megapascals (Young's modulus) was determined for all bone samples immediately before applying each daily loading episode, using the in-built Zetos protocol (18) over a 16- to 18-day experimental period, as indicated. This consisted of applying a 10-N preload to the bone cores and then increasing loading to a maximum of 4,000 microstrain, acquiring 50 measurements of deformation. An additional control group of bone cores (unloaded control) was cultured identically to the other groups but without either loading or the addition of rhSCL.

**Biochemical analyses.** The ionized calcium concentrations in the culture media were measured using a micro calcium ion electrode (Lazar Research Laboratories) and a direct UV method (10), respectively, as per manufacturer's instructions (ThermoFisher Scientific). The absorbance at 650 nm and 340 nm was measured on a Konelab 30 (ThermoFisher Scientific), respectively. Levels of COOH-terminal telopeptide of type I collagen (β-CTX) in the culture media were measured by enzyme-linked immunosorbent assay (ELISA) (Immunodiagnostic Systems, Boldon, UK).

**Bone histology.** Specimens for histology were fixed with 10% formalin (Asia Pacific Specialty Chemicals) and decalcified with PBS (pH 8.0) including 1% ethylenediaminetetraacetic acid (EDTA) disodium salt (Chem-Supply) and 0.5% paraformaldehyde (PFA; ThermoFisher Scientific) to decalcify samples slowly for tartrate-resistant acid phosphatase (TRAP) conservation. The samples were infiltrated and embedded in paraffin after decalcification. Sections, 5 μm thick, were stained by hematoxylin-eosin (H&E), toluidine blue, and TRAP staining. Images were captured by a Leica DM6000B microscope (Leica Microsystems, Wetzlar, Germany). Toluidine blue-stained sections were used to measure osteocyte lacuna size, which was quantified from images using a Quantimet imaging system (Leica) and ImageJ software, as de-

Table 1. Sequences of oligonucleotide primers for real-time RT-PCR designed on the basis of published bovine gene sequences and predicted PCR product sizes

| Target Gene  | Sense | Primer Sequence (5'→3')   | Expected Product Size, bp |
|--------------|-------|---------------------------|---------------------------|
| <i>BACT</i>  | S     | ACCGTGAGAAGATGACCCAGA     | 127                       |
|              | AS    | TCACCGGAGTCCATCAGC        |                           |
| <i>SOST</i>  | S     | CCCTTTGAGACCAAGAGCGC      | 244                       |
|              | AS    | CAGGACACAACAGCTGCACC      |                           |
| <i>CA2</i>   | S     | GGAAGAAATATGCTGCCGAGC     | 194                       |
|              | AS    | GAAGTCCGGTCTCTTACCCCTTTG  |                           |
| <i>TRAP</i>  | S     | GCAGCCAAGGAGGACTAGTG      | 176                       |
|              | AS    | CCATTCTCATCTGAAGGTAAGTGC  |                           |
| <i>CTSK</i>  | S     | CCTATCCATATGTTGGACAGGATG  | 169                       |
|              | AS    | AAGGAGGTCAGGCTTGCATC      |                           |
| <i>RANKL</i> | S     | CTACTTCGGAGGACAGTGG       | 90                        |
|              | AS    | TCCGTGTTTTTTCATGGAGCTTG   |                           |
| <i>MEPE</i>  | S     | TGACCCCTGGCAGCACCAAC      | 219                       |
|              | AS    | GCTCTTGACTTCTCTTGCCAGAATG |                           |
| <i>PHEX</i>  | S     | GGGTGTTCCGATGGGCCCTTA     | 217                       |
|              | AS    | ATACTTGCCGGTTTGCAGGA      |                           |

S, sense; AS, antisense.

scribed previously (23). These sections were also used to determine the percentage of occupied osteocyte lacunae, according to the number of visible nuclei, stained purple and located within the lacunae (35).

To visualize the calcium incorporation, bone cores were incubated with medium containing 3  $\mu\text{g/ml}$  calcein (Sigma Chemical, St. Louis, MO) for 24 h on *days 7* and *13* of the experiment. Specimens were fixed and embedded in methylmethacrylate. Bone blocks were trimmed and sectioned by microtome (Polycut-E, Leica SP 2600, Cambridge Instruments, Cambridge, UK). Calcein-labeled regions were imaged using the Quantimet (Leica) and the degree of calcein staining was also measured at 9–17 regions of each section, in 3–5 samples for each treatment. Fluorescence intensity was quantified using ImageJ software.

**Osteocyte-like cell cultures.** Human primary osteoblast-like cells were isolated from femoral trabecular bone taken from patients undergoing primary total hip replacement surgery and cultured *ex vivo*, as described previously (3). Samples were obtained with written, informed consent and approval by the Human Ethics Committee of the Royal Adelaide Hospital. Cells were cultured under differentiating conditions for a period of 28 days, which gives rise to cells that phenotypically resemble mature osteocytes (2, 4, 23, 35). Mature osteocyte-like cells were cultured for a further 72 h, either untreated or with the addition of rhSCL, as indicated. Supernatants were assayed for  $\beta$ -CTX levels, as above.

**RNA extraction and real-time polymerase chain reaction (PCR).** Extraction of RNA from bone and real-time RT-PCR was conducted, as described previously (23) with some modifications. Briefly, following the experimental protocol (*ex vivo* culture with or without mechanical loading or in the additional presence of rhSCL) bovine trabecular bone samples were rinsed in PBS, and cut into small pieces using sterile instruments cleaned with diethylpyrocarbonate (DEPC)-treated water. Trizol reagent (Life Technologies, Gaithersburg, MD) was added and the bone pieces were transferred to sterile 1.5-ml centrifuge tubes and further crushed using the blunt end of a pair of surgical steel scissors. The samples were frozen at  $-80^{\circ}\text{C}$  overnight, then thawed and centrifuged at 1,000 *g* for 5 min to pellet any insoluble material. Total RNA was then isolated as per manufacturer's instructions (Life Technologies). Complementary DNA (cDNA) was synthesized using iScript reagent (Bio-Rad Laboratories, Hercules, CA), and gene expression was analyzed by real-time RT-PCR using the SYBR Green incorporation technique. Relative gene expression between samples was calculated using the comparative cycle threshold method, using bovine actin-beta (ACTB) as a housekeeping gene. Oligonucleotide primers were designed in-house to flank intron-exon boundaries, and were purchased from Geneworks (Thebarton). Sequences of oligonucleotide primers used are shown in Table 1.

**Statistical analysis.** Statistical differences between data sets were assessed using one-way analysis of variance (ANOVA) followed by

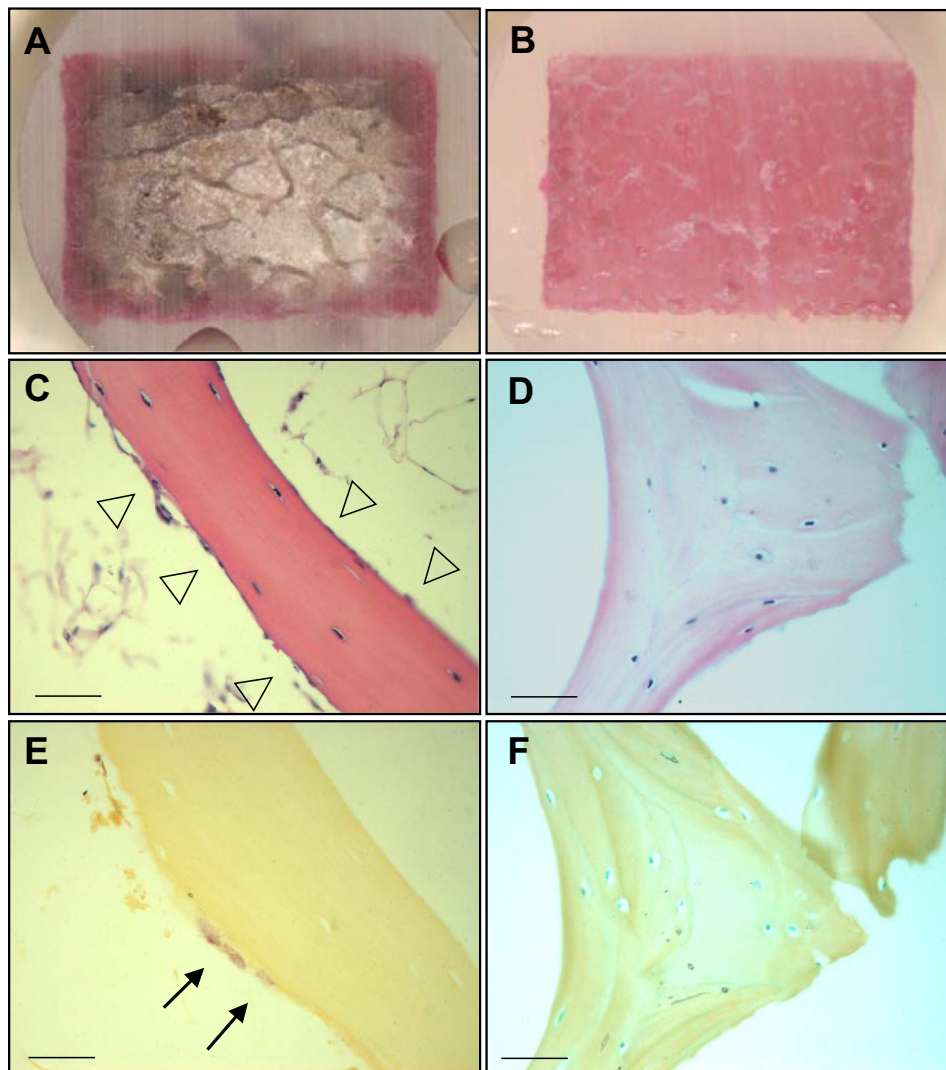


Fig. 1. The effect of bone marrow on perfusion. Bone cores with and without bone marrow ( $n = 3/\text{group}$ ) were seated in individual chambers and continuously perfused with media including Reactive red 120 for 24 h. Sagittal sections were obtained through the center of the bone cores with bone marrow (A) and without bone marrow (B). Specimens with and without bone marrow were fixed in 10% formaldehyde and decalcified with phosphate-buffered saline (pH 8.0) including 1% EDTA and 0.5% PFA, and cut into 5- $\mu\text{m}$ -thick sections. Samples stained with H&E and TRAP with bone marrow (C and E) and without bone marrow (D and F). Arrowheads indicate osteoblasts and lining cells. Arrows indicate TRAP-positive osteoclasts. Scale bar, 200  $\mu\text{m}$ .

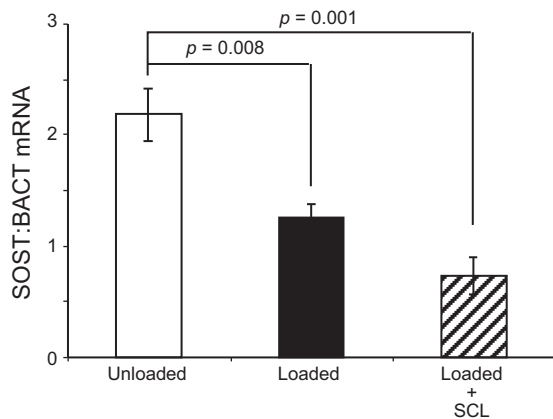


Fig. 2. *SOST* mRNA expression in response to loading in the presence or absence of rhSCL. Bone cores were divided into 3 groups: unloaded, loaded, and loaded in the presence 50 ng/ml of rhSCL over 7 days. Total RNA of bone was extracted and real-time RT-PCR was performed for *SOST* mRNA. Data are mean mRNA levels normalized to *BACT* mRNA  $\pm$  SD of triplicate wells. Significant difference from the unloaded control is indicated.

Tukey's post hoc test (GraphPad Prism). A value for  $P < 0.05$  was considered significant.

## RESULTS

**Bone organ culture.** The Zetos system comprises a piezoelectric controlled bone loading device, together with a continuous flow chamber that perfuses bone samples with culture medium to maintain bone viability (12). Since the Zetos device allows controlled physiological loading to be applied to large animal trabecular bone, we considered it a suitable system, in which to investigate the effects of sclerostin on mineral accrual induced by mechanical loading. Since we have established that osteocytes are target cells for the action of sclerostin (2, 23, 54), we first performed a control experiment to test whether osteocytes would be exposed to the perfusate. Bone cores with either an intact marrow or with marrow physically removed using a dental flossing device were perfused with Reactive Red 120 stain solution. After perfusion for 24 h, the bone cores were sectioned transversely and longitudinally. Poor dye penetration in bone cores with intact marrow suggested that perfusion was limited to the periphery (Fig. 1A), whereas complete dye penetration in cores with marrow removed showed that cores were perfused throughout (Fig. 1B). Marrow was therefore removed for all subsequent experiments. Histological analysis indicated that the flushing of bone marrow resulted in the removal of most bone lining cells, osteoblasts (Fig. 1C) and osteoclasts (Fig. 1E), with a significant enrichment of osteocytes in the bone cores (Fig. 1, D and F).

**The effect of mechanical loading on *SOST* mRNA expression.** The expression of sclerostin in bone is reported to be influenced by the local strain perceived by osteocytes, with low expression under load and higher expression in the unloaded state (31, 32, 45). This has mainly been examined in cortical bone in mice. Thus we sought to test whether loading of large animal trabecular bone also regulates endogenous *SOST* mRNA levels. Bone cores were divided into three groups, unloaded, loaded, and loaded with rhSCL (50 ng/ml) for periods of 4 h and 7 days, and mRNA of each sample was prepared for RT-PCR analysis. We observed that 4 h after a

single period of mechanical loading there was a trend for decreased *SOST* mRNA expression in comparison to unloaded bone (data not shown), and after 7 consecutive days of daily loading *SOST* expression was reduced by approximately half compared with unloaded bone samples (Fig. 2). The addition of exogenous rhSCL had no additional effect on the reduction of *SOST* mRNA expression in loaded bone.

**Effect of sclerostin on loading-induced stiffness.** It has been demonstrated previously in the Zetos system that loading changes the mechanical properties of the bone (11, 13, 53). To elucidate the direct effects of sclerostin on the loading response, cores were perfused with medium alone or medium containing added recombinant sclerostin, and mechanical load was applied daily. A third group of cores were cultured without daily loading or the addition of rhSCL. The stiffness (Young's modulus) of each bone core was determined each day and in the case of the loaded groups, before applying mechanical load. The apparent stiffness in the unloaded group increased slightly with time, as reported previously (13, 53). In response to daily loading, the apparent stiffness increased to a greater extent throughout the experimental period (Fig. 3), as reported previously (13, 53). However, the effect of loading was significantly abrogated by rhSCL treatment. These data show that sclerostin could attenuate the response to bone loading, most likely by a direct effect on osteocytes.

**Ionic calcium levels in culture media.** We have recently reported that rhSCL promotes osteocyte-mediated release of calcium from bone (23). To investigate whether these effects of sclerostin could occur in the context of mechanical loading, changes in the ionic calcium levels of the culture media were measured for each individual bone core. There was no detectable difference between groups during the first 2 wk of observation (data not shown), perhaps because of the relatively large volume of media perfused (7 ml) and the relatively short period (24 h), over which each sample was collected. However, media from the loaded + rhSCL group collected in the third week of culture showed significantly increased ionic cal-

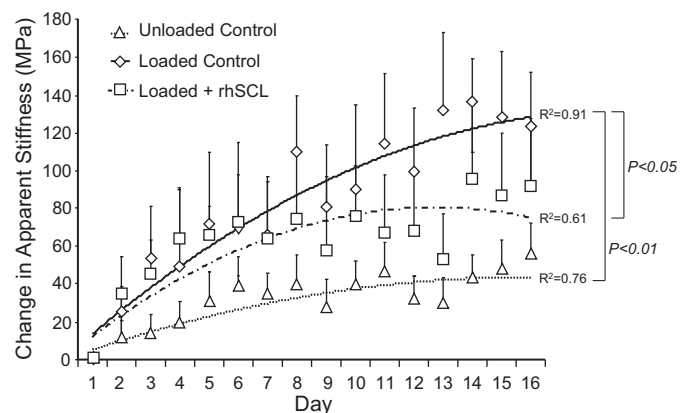


Fig. 3. Effects of sclerostin on apparent stiffness. The bone cores were divided into 3 groups: unloaded controls, loaded controls, and loaded + rhSCL (50 ng/ml). The loading procedure was 300 cycles/day of 2,000 microstrain applied at a frequency of 1 Hz for 3 wk. The apparent stiffness of each bone sample was determined daily immediately before the load was applied as described in MATERIALS AND METHODS. Data are means  $\pm$  SE of 8 samples per group, all obtained from the same bovine sternum. Similar data were obtained from 3 independent experiments. The regression coefficients ( $R^2$ ) for each group and significant difference between the groups are indicated.

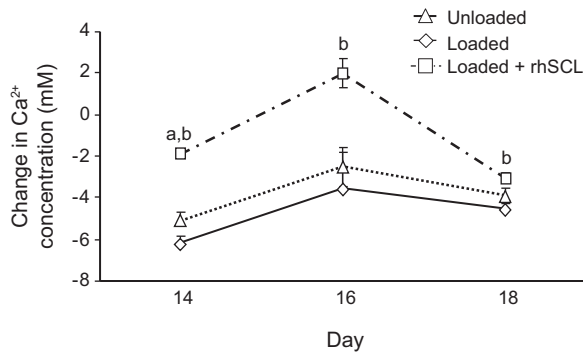


Fig. 4. Effects of mechanical stimulation and rhSCL on calcium concentration in the culture medium. Ionic calcium in the culture media was measured 24 h after loading or an equivalent time point for the unloaded control group. Data are means  $\pm$  SE (8 samples per group) of the change in calcium concentration during 1 day culture; significant differences: <sup>a</sup>between rhSCL group and unloaded Controls; <sup>b</sup>between rhSCL group and loaded Controls ( $P < 0.05$ ).

cium levels compared with the loaded and unloaded control samples (Fig. 4).

**Calcein incorporation.** We reported that treatment of human mineralizing osteocyte-like cultures with rhSCL *in vitro* resulted in the inhibition of mineral incorporation into the cell layer (2). To test the effect of sclerostin on mineral accrual in the bone cores, calcein was added to perfusates on *days 7* and *13* for a period of 24 h in each case and the bone cores processed for analysis after the 16-day experiment. Calcein was incorporated into the trabecular bone surfaces in all groups (Fig. 5). The overall fluorescence intensity of the loaded bone cores was significantly higher than that in the unloaded group, indicative of increased dynamic calcium uptake in response to loading (Fig. 5D). The incorporation of calcein into the bone cores in the presence of rhSCL (Fig. 5B) was significantly lower than in the cores perfused with medium alone (Fig. 5A).

Higher power microscopy revealed that calcein labeling was most prominent on the surfaces of bone, including those of vascular pores, and within osteocyte lacunae (Fig. 5C), the latter consistent with osteocytes directly regulating perilacunar mineral in this system.

**Histology.** As stated, the predominant cell type remaining in the trabecular bone cores after flushing was osteocytes (Fig. 1D) and this remained the case after of culture *ex vivo*, with histological analysis revealing an apparent absence of both TRAP-positive osteoclasts (not shown) and osteoblasts (Fig. 6A). Osteocytes showed an evenly spread, noncondensed nucleus, consistent with cell viability, with the cell body often positioned eccentrically within the lacunae (Fig. 6A). To determine the viability of the remaining osteocytes, we measured the osteocyte lacunar occupancy. There was  $\sim 80\%$  occupancy of osteocyte lacunae overall, with no significant differences observed between groups (Fig. 6B). Analysis revealed that the size of lacunae increased significantly with rhSCL treatment, in comparison to the cores perfused in medium alone, either loaded or unloaded (Fig. 6C).

**The effect of sclerostin on markers of bone resorption and formation.** To investigate bone resorption in this system, we analyzed the culture media for the presence of carboxy-terminal cross-linking telopeptides of type I collagen ( $\beta$ -CTX).  $\beta$ -CTX levels decreased after the first week of culture, and increased thereafter (Fig. 6D). After prolonged culture, the level of  $\beta$ -CTX was significantly elevated in the presence of rhSCL, compared with either unloaded or loaded control cores, suggesting that rhSCL could enhance the degradation of the bone matrix. The absence of observable osteoclasts implied that osteocytes were mediating this process. To test this, we generated human primary osteocyte-like cultures, consisting of differentiated cells residing in an endogenous mineralized type I collagen matrix (2, 4, 23, 35), and treated these cells for 72

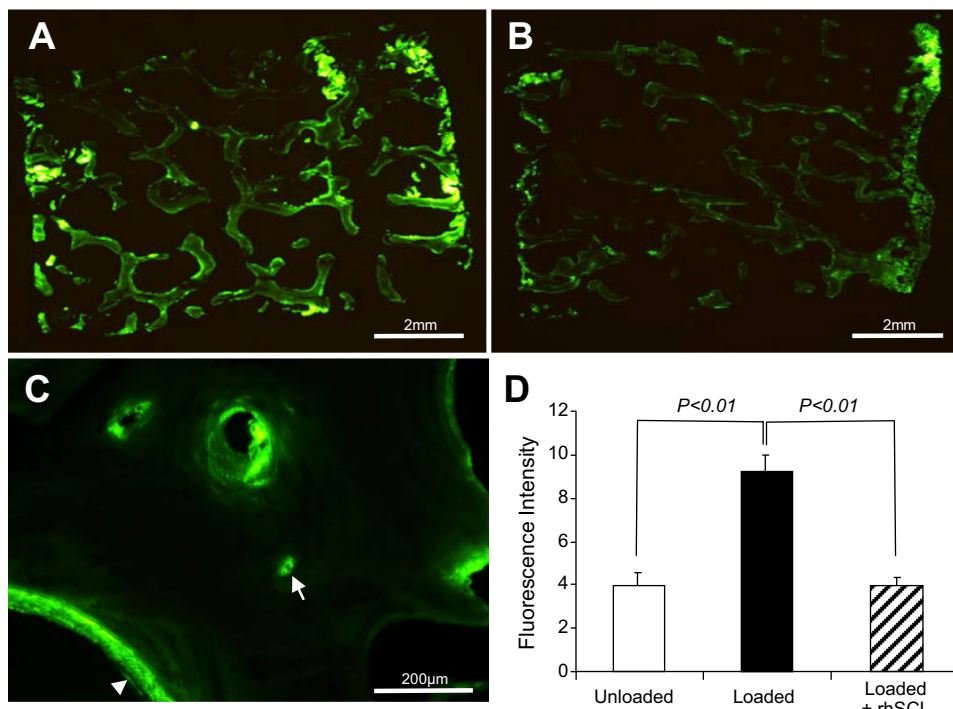


Fig. 5. Effects of rhSCL on bone mineralization. Bovine bone cores were perfused with calcein and processed for sectioning as described in MATERIALS AND METHODS. *A*: a cross section of a whole bone core (dimensions 10 mm  $\times$  5 mm) cultured with daily mechanical loading. *B*: an example of a bone core loaded in the presence of rhSCL. *C*: labeling at a higher magnification (20 $\times$  objective) showing an example of calcein labeling at the trabecular surface (arrowhead) and a labeled osteocyte lacuna (arrow). *D*: quantification of total calcein labeling; data shown are means of fluorescence intensity  $\pm$  SE.  $n = 5$  bone cores group, all obtained from the same bovine sternum. Similar results were obtained for 2 independent experiments.

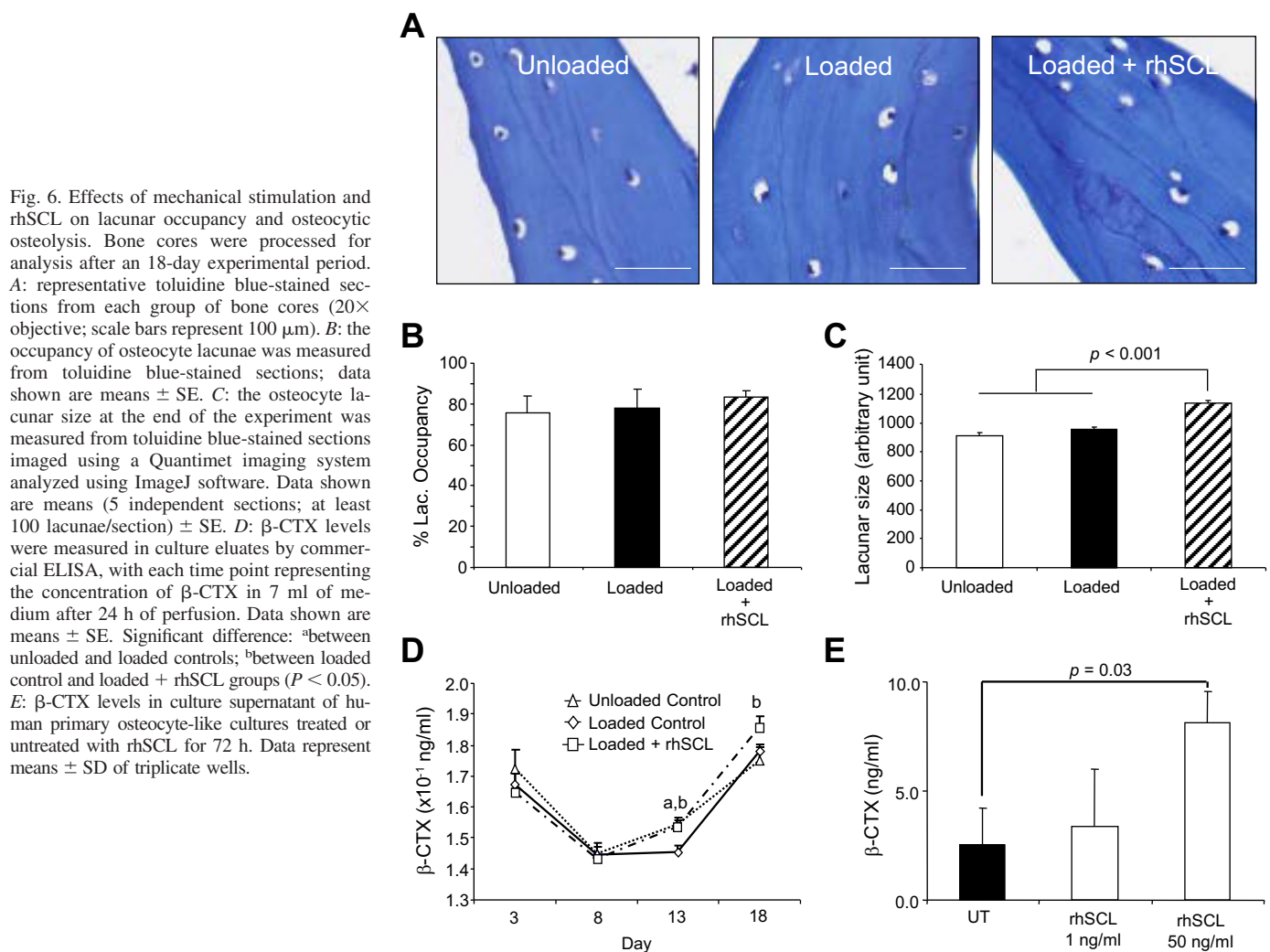


Fig. 6. Effects of mechanical stimulation and rhSCL on lacunar occupancy and osteocytic osteolysis. Bone cores were processed for analysis after an 18-day experimental period. **A**: representative toluidine blue-stained sections from each group of bone cores (20 $\times$  objective; scale bars represent 100  $\mu$ m). **B**: the occupancy of osteocyte lacunae was measured from toluidine blue-stained sections; data shown are means  $\pm$  SE. **C**: the osteocyte lacunar size at the end of the experiment was measured from toluidine blue-stained sections imaged using a Quantimet imaging system analyzed using ImageJ software. Data shown are means (5 independent sections; at least 100 lacunae/section)  $\pm$  SE. **D**:  $\beta$ -CTX levels were measured in culture eluates by commercial ELISA, with each time point representing the concentration of  $\beta$ -CTX in 7 ml of medium after 24 h of perfusion. Data shown are means  $\pm$  SE. Significant difference: <sup>a</sup>between unloaded and loaded controls; <sup>b</sup>between loaded control and loaded + rhSCL groups ( $P < 0.05$ ). **E**:  $\beta$ -CTX levels in culture supernatant of human primary osteocyte-like cultures treated or untreated with rhSCL for 72 h. Data represent means  $\pm$  SD of triplicate wells.

h with rhSCL. As shown in Fig. 6E, measurably increased  $\beta$ -CTX was released into the culture supernatant in response to rhSCL at 50 ng/ml.

To investigate the effect of sclerostin on resorption marker gene expression, we cultured bone cores for 3 days with rhSCL at concentrations from 1 to 50 ng/ml. Consistent with our findings in human osteocyte-like cells, MLO-Y4 osteocytes and in human trabecular bone (23, 54), rhSCL induced the mRNA expression of the resorption-associated genes *TRAP*, cathepsin K, and *RANKL* (Fig. 7, A–D). Recombinant human sclerostin treatment also induced the expression of the mineralization inhibitory gene *MEPE* in a dose-dependent manner (Fig. 7E) and decreased the expression of the mineralization promoting gene, phosphate regulating gene with homologies to endopeptidases on the X-chromosome (*PHEX*), at concentrations between 1 and 50 ng/ml (Fig. 7F), consistent with our findings in osteocytes in vitro and ex vivo (2).

## DISCUSSION

Accumulating evidence indicates that sclerostin, which is predominantly secreted from mature osteocytes, is a local regulator of bone metabolism. Osteocytes, including preosteocytes, constitute the major cell type in bone and are likely targets for the activity of sclerostin, based both on in vitro studies that demonstrate osteocyte sensitivity to sclerostin and its very localized and regulated expression pattern in bone (2, 23, 54). The expression of sclerostin appears to reflect local strains perceived by osteocytes, with low production under mechanical load and high production in the unloaded condition (31, 32, 45). Sclerostin is known to negatively regulate bone mass by inhibiting the Wntless integration (Wnt)/ $\beta$ -catenin pathway. Javaheri and colleagues (17) showed that bone formation induced by mechanical loading did not occur in mice lacking an allele of the  $\beta$ -catenin gene, indicating the importance of the Wnt/ $\beta$ -catenin signaling pathway for the effect of loading. Furthermore, transgenic expression of *SOST* also antagonized loading-induced bone formation in mice (49). However, the function of sclerostin in mechanical loading has been less well characterized in trabecular bone, particularly from large animals. Here, we sought to determine the effect of exogenous sclerostin on the response of bovine cancellous bone to daily episodes of loading. We used a concentration of rhSCL that we showed previously was near maximal for its effects on human osteocytes in vitro (2, 54). Although this is ~50–60-fold higher than levels typically found in the circula-

tes, constitute the major cell type in bone and are likely targets for the activity of sclerostin, based both on in vitro studies that demonstrate osteocyte sensitivity to sclerostin and its very localized and regulated expression pattern in bone (2, 23, 54). The expression of sclerostin appears to reflect local strains perceived by osteocytes, with low production under mechanical load and high production in the unloaded condition (31, 32, 45). Sclerostin is known to negatively regulate bone mass by inhibiting the Wntless integration (Wnt)/ $\beta$ -catenin pathway. Javaheri and colleagues (17) showed that bone formation induced by mechanical loading did not occur in mice lacking an allele of the  $\beta$ -catenin gene, indicating the importance of the Wnt/ $\beta$ -catenin signaling pathway for the effect of loading. Furthermore, transgenic expression of *SOST* also antagonized loading-induced bone formation in mice (49). However, the function of sclerostin in mechanical loading has been less well characterized in trabecular bone, particularly from large animals. Here, we sought to determine the effect of exogenous sclerostin on the response of bovine cancellous bone to daily episodes of loading. We used a concentration of rhSCL that we showed previously was near maximal for its effects on human osteocytes in vitro (2, 54). Although this is ~50–60-fold higher than levels typically found in the circula-

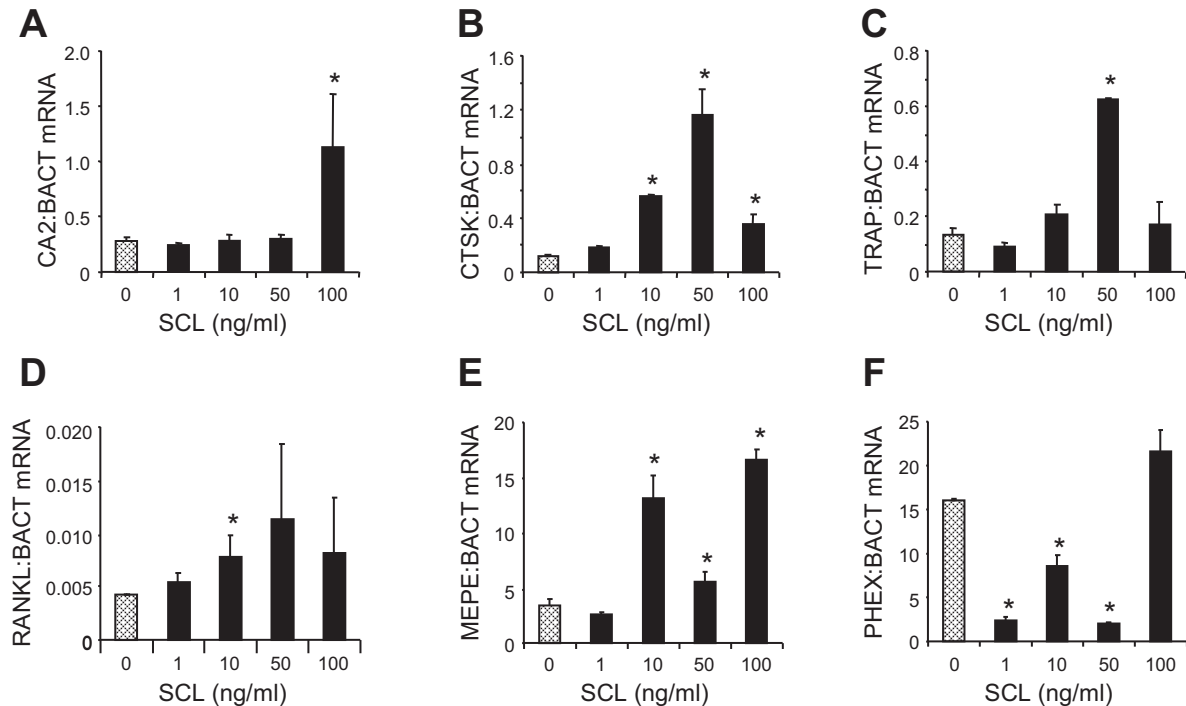


Fig. 7. Effects of sclerostin on gene expression. Bovine trabecular bone was prepared as described in MATERIALS AND METHODS and cultured ex vivo (without loading) with different doses of rhSCL (0–100 ng/ml). Total RNA was extracted at 72 h and real-time RT-PCR performed for *CA2* (A), *CTSK* (B), *TRAP* (C), *RANKL* (D), *MEPE* (E), and *PHEX* mRNA (F). Data are mean expressions normalized to that of the housekeeping gene *BACT* mRNA  $\pm$  SD for triplicate RT-PCR reactions from quadruplicate bone samples/group. Difference in expression from the untreated control is indicated (\* $P < 0.05$ ).

tion, the local bone fluid concentration of sclerostin deriving from osteocytes, and to which the responding cells are exposed, is unknown but is likely to be considerably higher than the circulating level. Consistent with previous reports using a similar system (13, 53), we observed a significant increase in stiffness in cyclically loaded bovine trabecular bone ex vivo compared with baseline and to identically cultured unloaded controls. In the present study, this was observed in a reductionist system, with removal of bone marrow and detectable bone surface cells, and in the absence of functional vasculature, neural, and endocrine systems. Furthermore, suppression of endogenous *SOST* mRNA expression in response to load was observed, at least over the first 7 days, consistent with in vivo models (31, 32, 45). Notably, perfusion of bone with rhSCL suppressed the positive effect of mechanical loading on bone stiffness.

In seeking a mechanistic explanation for changes in stiffness, we observed, using a calcein surrogate as a marker, a decreased uptake of calcium in bone loaded in the presence of exogenous rhSCL compared with loaded control samples. It is likely that additional mineralization within the bone matrix had a measurable effect on the stiffness of the bone cores, since bone mineralization and modulus have been shown to be positively correlated (14). Parfitt (37) reviewed the literature relating to calcium exchange between the bone and the extracellular fluid, citing experiments using radiolabeled calcium, which showed “immediate rapid uptake at all bone surfaces accessible to the circulation, regardless of their cellular activity or degree of mineralisation.” This is consistent with the common observation that bone explants in culture take up calcium from the medium, likely by simple physicochemical mecha-

nisms. Parfitt (37) described a pool of calcium that is exchangeable with bone surfaces, and it has subsequently been experimentally demonstrated that an osteocyte-mediated mechanism, driven for example by parathyroid hormone (PTH) (39), can mobilize calcium (and phosphate) from this pool into the circulation. Calcium uptake into bone may therefore proceed by a simple physicochemical mechanism, with its release being controlled by osteocytes, which are in turn regulated by mediators, such as PTH and, as we have shown previously (2), sclerostin. This mechanism relies on viable osteocytes and it has been shown that osteocyte death is associated with mineralizing osteocyte lacunae (6, 7).

We have recently demonstrated that rhSCL induced the expression by osteocytes of a number of mediators previously associated with bone resorption by osteoclasts. These included RANKL, carbonic anhydrase 2, cathepsin K, and TRAP (23). A similar panel of genes was shown to be associated with osteocytic osteolysis during lactation (41). We have identified that sclerostin also regulates osteocyte-mediated bone mineralization through regulation of the PHEX/MEPE axis, and that the upregulation by sclerostin of MEPE and MEPE-ASARM peptides was critical to the inhibitory effect of sclerostin (2). Sclerostin treatment of bovine bone upregulated the expression of *MEPE* mRNA and inhibited the expression of *PHEX* mRNA, consistent with our report in human bone (2). The combined regulation of these mineralization-associated proteins by sclerostin could provide cell-mediated control of the perilacunar mineralization and serve as a prelude to removal of the organic matrix, the latter evidenced by the release of  $\beta$ -CTX from the bone cores. Strong confirmatory evidence for this was obtained using differentiated cultures of human pri-

mary osteocyte-like cells, where we show for the first time the release of  $\beta$ -CTX by the activity of osteocytes in response to sclerostin. This is consistent with, and appears to result in, the enlargement of the osteocyte lacuna size in the rhSCL-treated bone. This is also consistent with our previous observations of the effect of sclerostin in human trabecular bone (23), and provides the first direct evidence that sclerostin can effect collagen breakdown by its actions on osteocytes and can do so even when trabecular bone is mechanically loaded. Interestingly, the osteocyte lacunar size in loaded + rhSCL-treated samples was significantly larger than that in both loaded and unloaded groups, and indeed there was no difference in this parameter in these two groups, consistent with the reports by others that significant osteocytic osteolysis does not seem to occur in response to mechanical unloading (29, 41). On the other hand, dramatic changes in osteocyte morphology occurred after spinal cord injury in rats, which could be prevented by treatment with neutralizing sclerostin antibodies (40). It appears that altered lacunocanalicular morphology has implications for the mechanical properties of bone. For example, it was elegantly shown in lactating rats that the bone elastic modulus decreased inversely with the increase in osteocyte lacunocanalicular porosity (19), consistent with the reduced gain in modulus seen in the present experiments with rhSCL treatment. Thus it is conceivable that the mechanical loading-induced reduction of endogenous sclerostin expression serves to stabilize the perilacunar matrix.

In summary, we propose that our observations are consistent with the notion of passive uptake by bone of calcium, which is maintained in balance by osteocytes, and that loading results in increased mineral incorporation into the periosteocyte matrix. Sclerostin, by an as yet undetermined mechanism, causes the release by osteocytes of bone matrix resorptive molecules, thereby reducing the effects of loading on mineral accrual. It is not known whether these experimental observations with exogenous sclerostin are reflective of physiological or pathological processes. However, increased levels of sclerostin in bone, as might be caused by inflammation (52) for example, could reduce the anabolic effects of mechanical loading. The contribution of osteocytes to circulating  $\beta$ -CTX, a major serum bone turnover marker, in vivo is an interesting area of future research. Our findings are of potential relevance to the mechanism of action of sclerostin-targeting therapies, since  $\beta$ -CTX levels are strongly suppressed in individuals receiving sclerostin-neutralizing antibodies (36, 43).

#### ACKNOWLEDGMENTS

We thank Dr. Everett Smith (Univ. of Wisconsin) for help in establishing the Zetos device.

#### GRANTS

This work was funded by National Health and Medical Research Council of Australia (NHMRC) Project Grant Scheme (Grant No. 1004871). G. J. Atkins is a NHMRC Senior Research Fellow.

#### DISCLOSURES

No conflicts of interest, financial or otherwise, are declared by the authors.

#### AUTHOR CONTRIBUTIONS

D.M.F. and G.J.A. conceived and designed research; M.K., K.A.K., A.R.W., and R.T.O. performed experiments; M.K., K.A.K., A.R.W., R.T.O., P.H.A., and G.J.A. analyzed data; M.K., A.R.W., A.E., P.H.A., D.M.F., and

G.J.A. interpreted results of experiments; M.K., R.T.O., and G.J.A. prepared figures; M.K., R.T.O., D.M.F., and G.J.A. drafted manuscript; A.E., P.H.A., D.M.F., and G.J.A. edited and revised manuscript; M.K., K.A.K., A.R.W., R.T.O., A.E., P.H.A., D.M.F., and G.J.A. approved final version of manuscript.

#### REFERENCES

- Atkins GJ, Findlay DM. Osteocyte regulation of bone mineral: a little give and take. *Osteoporos Int* 23: 2067–2079, 2012. doi:10.1007/s00198-012-1915-z.
- Atkins GJ, Rowe PS, Lim HP, Weldon KJ, Ormsby R, Wijenayaka AR, Zelenchuk L, Evdokiou A, Findlay DM. Sclerostin is a locally acting regulator of late-osteoblast/preosteocyte differentiation and regulates mineralization through a MEPE-ASARM-dependent mechanism. *J Bone Miner Res* 26: 1425–1436, 2011. doi:10.1002/jbmr.345.
- Atkins GJ, Weldon KJ, Halbout P, Findlay DM. Strontium ranelate treatment of human primary osteoblasts promotes an osteocyte-like phenotype while eliciting an osteoprotegerin response. *Osteoporos Int* 20: 653–664, 2009. doi:10.1007/s00198-008-0728-6.
- Atkins GJ, Weldon KJ, Wijenayaka AR, Bonewald LF, Findlay DM. Vitamin K promotes mineralization, osteoblast-to-osteocyte transition, and an anticatabolic phenotype by gamma-carboxylation-dependent and -independent mechanisms. *Am J Physiol Cell Physiol* 297: C1358–C1367, 2009. doi:10.1152/ajpcell.00216.2009.
- Aw MS, Khalid KA, Gulati K, Atkins GJ, Pivonka P, Findlay DM, Losic D. Characterization of drug-release kinetics in trabecular bone from titania nanotube implants. *Int J Nanomedicine* 7: 4883–4892, 2012. doi:10.2147/IJN.S33655.
- Bell LS, Kayser M, Jones C. The mineralized osteocyte: a living fossil. *Am J Phys Anthropol* 137: 449–456, 2008. doi:10.1002/ajpa.20886.
- Busse B, Djonic D, Milovanovic P, Hahn M, Püschel K, Ritchie RO, Djuric M, Amling M. Decrease in the osteocyte lacunar density accompanied by hypermineralized lacunar occlusion reveals failure and delay of remodeling in aged human bone. *Aging Cell* 9: 1065–1075, 2010. doi:10.1111/j.1474-9726.2010.00633.x.
- Chen JH, Liu C, You L, Simmons CA. Boning up on Wolff's Law: mechanical regulation of the cells that make and maintain bone. *J Biomech* 43: 108–118, 2010. doi:10.1016/j.jbiomech.2009.09.016.
- Choi HY, Dieckmann M, Herz J, Niemeier A. Lrp4, a novel receptor for Dickkopf 1 and sclerostin, is expressed by osteoblasts and regulates bone growth and turnover in vivo. *PLoS One* 4: e7930, 2009. doi:10.1371/journal.pone.0007930.
- Daly JA, Ertingshausen G. Direct method for determining inorganic phosphate in serum with the "CentrifChem". *Clin Chem* 18: 263–265, 1972.
- David V, Guignandon A, Martin A, Malaval L, Lafage-Proust MH, Rattner A, Mann V, Noble B, Jones DB, Vico L. Ex Vivo bone formation in bovine trabecular bone cultured in a dynamic 3D bioreactor is enhanced by compressive mechanical strain. *Tissue Eng Part A* 14: 117–126, 2008. doi:10.1089/ten.a.2007.0051.
- Davies CM, Jones DB, Stoddart MJ, Koller K, Smith E, Archer CW, Richards RG. Mechanically loaded ex vivo bone culture system "Zetos": systems and culture preparation. *Eur Cell Mater* 11: 57–75, 2006. doi:10.22203/eCM.v011a07.
- Endres S, Kratz M, Wunsch S, Jones DB. Zetos: a culture loading system for trabecular bone. Investigation of different loading signal intensities on bovine bone cylinders. *J Musculoskelet Neuronal Interact* 9: 173–183, 2009.
- Follet H, Boivin G, Rumelhart C, Meunier PJ. The degree of mineralization is a determinant of bone strength: a study on human calcanei. *Bone* 34: 783–789, 2004. doi:10.1016/j.bone.2003.12.012.
- Fritton SP, Weinbaum S. Fluid and solute transport in bone: flow-induced mechanotransduction. *Annu Rev Fluid Mech* 41: 347–374, 2009. doi:10.1146/annurev.fluid.010908.165136.
- Henriksen K, Neutsky-Wulff AV, Bonewald LF, Karsdal MA. Local communication on and within bone controls bone remodeling. *Bone* 44: 1026–1033, 2009. doi:10.1016/j.bone.2009.03.671.
- Javaheri B, Stern AR, Lara N, Dallas M, Zhao H, Liu Y, Bonewald LF, Johnson ML. Deletion of a single  $\beta$ -catenin allele in osteocytes abolishes the bone anabolic response to loading. *J Bone Miner Res* 29: 705–715, 2014. doi:10.1002/jbmr.2064.
- Jones DB, Broeckmann E, Pohl T, Smith EL. Development of a mechanical testing and loading system for trabecular bone studies for long term culture. *Eur Cell Mater* 5: 48–59, 2003. doi:10.22203/eCM.v005a05.

19. Kaya S, Basta-Pljakic J, Seref-Ferlengez Z, Majeska RJ, Cardoso L, Bromage TG, Zhang Q, Flach CR, Mendelsohn R, Yakar S, Fritton SP, Schaffler MB. Lactation-induced changes in the volume of osteocyte lacunar-canalicular space alter mechanical properties in cortical bone tissue. *J Bone Miner Res* 32: 688–697, 2017. doi:10.1002/jbmr.3044.
20. Klein-Nulend J, Bacabac RG, Mullender MG. Mechanobiology of bone tissue. *Pathol Biol (Paris)* 53: 576–580, 2005. doi:10.1016/j.patbio.2004.12.005.
21. Klein-Nulend J, Bonewald L. The osteocyte. In: *Principles of Bone Biology* (3rd ed.), edited by Bilezikian JP, Raisz LG, Martin TJ. San Diego, CA: Academic, 2008, p. 153–174. doi:10.1016/B978-0-12-373884-4.00028-8.
22. Knothe Tate ML, Adamson JR, Tami AE, Bauer TW. The osteocyte. *Int J Biochem Cell Biol* 36: 1–8, 2004. doi:10.1016/S1357-2725(03)00241-3.
23. Kogawa M, Wijenayaka AR, Ormsby RT, Thomas GP, Anderson PH, Bonewald LF, Findlay DM, Atkins GJ. Sclerostin regulates release of bone mineral by osteocytes by induction of carbonic anhydrase 2. *J Bone Miner Res* 28: 2436–2448, 2013. doi:10.1002/jbmr.2003.
24. Kogianni G, Noble BS. The biology of osteocytes. *Curr Osteoporos Rep* 5: 81–86, 2007. doi:10.1007/s11914-007-0007-z.
25. Krause C, Korchynski O, de Rooij K, Weidauer SE, de Gorter DJ, van Bezooijen RL, Hatsell S, Economides AN, Mueller TD, Löwik CW, ten Dijke P. Distinct modes of inhibition by sclerostin on bone morphogenetic protein and Wnt signaling pathways. *J Biol Chem* 285: 41614–41626, 2010. doi:10.1074/jbc.M110.153890.
26. Leupin O, Pitters E, Halleux C, Hu S, Kramer I, Morvan F, Bouwmeester T, Schirle M, Bueno-Lozano M, Fuentes FJ, Itin PH, Boudin E, de Freitas F, Jennes K, Brannetti B, Charara N, Ebersbach H, Geisse S, Lu CX, Bauer A, Van Hul W, Kneissel M. Bone overgrowth-associated mutations in the LRP4 gene impair sclerostin facilitator function. *J Biol Chem* 286: 19489–19500, 2011. doi:10.1074/jbc.M110.190330.
27. Li X, Zhang Y, Kang H, Liu W, Liu P, Zhang J, Harris SE, Wu D. Sclerostin binds to LRP5/6 and antagonizes canonical Wnt signaling. *J Biol Chem* 280: 19883–19887, 2005. doi:10.1074/jbc.M413274200.
28. Lin C, Jiang X, Dai Z, Guo X, Weng T, Wang J, Li Y, Feng G, Gao X, He L. Sclerostin mediates bone response to mechanical unloading through antagonizing Wnt/beta-catenin signaling. *J Bone Miner Res* 24: 1651–1661, 2009. doi:10.1359/jbmr.090411.
29. Lloyd SA, Loiselle AE, Zhang Y, Donahue HJ. Evidence for the role of connexin 43-mediated intercellular communication in the process of intracortical bone resorption via osteocytic osteolysis. *BMC Musculoskelet Disord* 15: 122, 2014. doi:10.1186/1471-2474-15-122.
30. Macias BR, Aspenberg P, Agholme F. Paradoxical *Sost* gene expression response to mechanical unloading in metaphyseal bone. *Bone* 53: 515–519, 2013. doi:10.1016/j.bone.2013.01.018.
31. Moustafa A, Sugiyama T, Prasad J, Zaman G, Gross TS, Lanyon LE, Price JS. Mechanical loading-related changes in osteocyte sclerostin expression in mice are more closely associated with the subsequent osteogenic response than the peak strains engendered. *Osteoporos Int* 23: 1225–1234, 2012. doi:10.1007/s00198-011-1656-4.
32. Moustafa A, Sugiyama T, Saxon LK, Zaman G, Sinters A, Armstrong VJ, Javaheri B, Lanyon LE, Price JS. The mouse fibula as a suitable bone for the study of functional adaptation to mechanical loading. *Bone* 44: 930–935, 2009. doi:10.1016/j.bone.2008.12.026.
33. Noble BS. The osteocyte lineage. *Arch Biochem Biophys* 473: 106–111, 2008. doi:10.1016/j.abb.2008.04.009.
34. Noble BS, Reeve J. Osteocyte function, osteocyte death and bone fracture resistance. *Mol Cell Endocrinol* 159: 7–13, 2000. doi:10.1016/S0303-7207(99)00174-4.
35. Ormsby RT, Cantley M, Kogawa M, Solomon LB, Haynes DR, Findlay DM, Atkins GJ. Evidence that osteocyte perilacunar remodelling contributes to polyethylene wear particle induced osteolysis. *Acta Biomater* 33: 242–251, 2016. doi:10.1016/j.actbio.2016.01.016.
36. Padhi D, Jang G, Stouch B, Fang L, Posvar E. Single-dose, placebo-controlled, randomized study of AMG 785, a sclerostin monoclonal antibody. *J Bone Miner Res* 26: 19–26, 2011. doi:10.1002/jbmr.173.
37. Parfitt AM. Misconceptions (3): calcium leaves bone only by resorption and enters only by formation. *Bone* 33: 259–263, 2003. doi:10.1016/j.bone.2003.05.002.
38. Poole KE, van Bezooijen RL, Loveridge N, Hamersma H, Papapoulos SE, Löwik CW, Reeve J. Sclerostin is a delayed secreted product of osteocytes that inhibits bone formation. *FASEB J* 19: 1842–1844, 2005.
39. Powell WF, Jr, Barry KJ, Tulum I, Kobayashi T, Harris SE, Bringhurst FR, Pajevic PD. Targeted ablation of the PTH/PTHrP receptor in osteocytes impairs bone structure and homeostatic calcemic responses. *J Endocrinol* 209: 21–32, 2011. doi:10.1530/JOE-10-0308.
40. Qin W, Li X, Peng Y, Harlow LM, Ren Y, Wu Y, Li J, Qin Y, Sun J, Zheng S, Brown T, Feng JQ, Ke HZ, Bauman WA, Cardozo CC. Sclerostin antibody preserves the morphology and structure of osteocytes and blocks the severe skeletal deterioration after motor-complete spinal cord injury in rats. *J Bone Miner Res* 30: 1994–2004, 2015. doi:10.1002/jbmr.2549.
41. Qing H, Ardeshirpour L, Pajevic PD, Dusevich V, Jähn K, Kato S, Wysolmerski J, Bonewald LF. Demonstration of osteocytic perilacunar/canalicular remodeling in mice during lactation. *J Bone Miner Res* 27: 1018–1029, 2012. doi:10.1002/jbmr.1567.
42. Razi H, Birkhold AI, Weinkamer R, Duda GN, Willie BM, Checa S. Aging leads to a dysregulation in mechanically driven bone formation and resorption. *J Bone Miner Res* 30: 1864–1873, 2015. doi:10.1002/jbmr.2528.
43. Recker RR, Benson CT, Matsumoto T, Bolognese MA, Robins DA, Alam J, Chiang AY, Hu L, Kregge JH, Sowa H, Mitlak BH, Myers SL. A randomized, double-blind phase 2 clinical trial of blosozumab, a sclerostin antibody, in postmenopausal women with low bone mineral density. *J Bone Miner Res* 30: 216–224, 2015. doi:10.1002/jbmr.2351.
44. Robling AG, Castillo AB, Turner CH. Biomechanical and molecular regulation of bone remodeling. *Annu Rev Biomed Eng* 8: 455–498, 2006. doi:10.1146/annurev.bioeng.8.061505.095721.
45. Robling AG, Niziolek PJ, Baldrige LA, Condon KW, Allen MR, Alam I, Mantila SM, Gluhak-Heinrich J, Bellido TM, Harris SE, Turner CH. Mechanical stimulation of bone in vivo reduces osteocyte expression of *Sost/sclerostin*. *J Biol Chem* 283: 5866–5875, 2008. doi:10.1074/jbc.M705092200.
47. Rubin J, Rubin C, Jacobs CR. Molecular pathways mediating mechanical signaling in bone. *Gene* 367: 1–16, 2006. doi:10.1016/j.gene.2005.10.028.
48. Spatz JM, Ellman R, Cloutier AM, Louis L, van Vliet M, Suva LJ, Dwyer D, Stolina M, Ke HZ, Bouxsein ML. Sclerostin antibody inhibits skeletal deterioration due to reduced mechanical loading. *J Bone Miner Res* 28: 865–874, 2013. doi:10.1002/jbmr.1807.
49. Tu X, Rhee Y, Condon KW, Bivi N, Allen MR, Dwyer D, Stolina M, Turner CH, Robling AG, Plotkin LI, Bellido T. *Sost* downregulation and local Wnt signaling are required for the osteogenic response to mechanical loading. *Bone* 50: 209–217, 2012. doi:10.1016/j.bone.2011.10.025.
50. Turner CH. Bone strength: current concepts. *Ann N Y Acad Sci* 1068: 429–446, 2006. doi:10.1196/annals.1346.039.
51. van Bezooijen RL, Svensson JP, Eefting D, Visser A, van der Horst G, Karperien M, Quax PH, Vrieling H, Papapoulos SE, ten Dijke P, Löwik CW. Wnt but not BMP signaling is involved in the inhibitory action of sclerostin on BMP-stimulated bone formation. *J Bone Miner Res* 22: 19–28, 2007. doi:10.1359/jbmr.061002.
52. Vincent C, Findlay DM, Welldon KJ, Wijenayaka AR, Zheng TS, Haynes DR, Fazzalari NL, Evdokiou A, Atkins GJ. Pro-inflammatory cytokines TNF-related weak inducer of apoptosis (TWEAK) and TNF $\alpha$  induce the mitogen-activated protein kinase (MAPK)-dependent expression of sclerostin in human osteoblasts. *J Bone Miner Res* 24: 1434–1449, 2009. doi:10.1359/jbmr.090305.
53. Vivanco J, Garcia S, Ploeg HL, Alvarez G, Cullen D, Smith EL. Apparent elastic modulus of ex vivo trabecular bovine bone increases with dynamic loading. *Proc Inst Mech Eng H* 227: 904–912, 2013. doi:10.1177/0954411913486855.
54. Wijenayaka AR, Kogawa M, Lim HP, Bonewald LF, Findlay DM, Atkins GJ. Sclerostin stimulates osteocyte support of osteoclast activity by a RANKL-dependent pathway. *PLoS One* 6: e25900, 2011. doi:10.1371/journal.pone.0025900.
55. Winkler DG, Sutherland MK, Geoghegan JC, Yu C, Hayes T, Skonier JE, Shpektor D, Jonas M, Kovacevich BR, Staehling-Hampton K, Appleby M, Brunkow ME, Latham JA. Osteocyte control of bone formation via sclerostin, a novel BMP antagonist. *EMBO J* 22: 6267–6276, 2003. doi:10.1093/emboj/cdg599.